Journal of Optoelectronics and Advanced Materials Vol. 7, No. 4, August 2005, p. 1915 - 1922

SIMULATIONAL ANALYSIS OF GLASSES PREPARED VIA DIFFERENT INTERATOMIC POTENTIALS

Y. Sano*, J. Kōga, F. Yonezawa

Department of Physics, Keio University, 3-14-1 Hiyoshi, Kohoku-ku,
Yokohama 223-8522 Japan

All glasses and amorphous solids have common characteristics; That is to say, they have no long-range order (LRO), but maintain the short-range order (SRO) reflecting the types of cohesion. In order to classify glasses beyond this common feature, therefore, it is necessary to introduce some other measure by which we can distinguish different atomic structures of glasses. Under this situation, it is the purpose of the present article to propose such a quantity. To this end, we first carry out, by means of molecular-dynamics (MD) method, rapid-quench simulations to construct glassy structures of the Lennard-Jones (LJ) systems and of the systems with the Stillinger-Weber (SW) potentials. Secondly, we evaluate several physical properties of the glasses thus obtained. Note that the crystalline phase of an LJ system is fcc which is the closest-packing structure, while that of an SW system is bcc where the atoms are more sparsed than in fcc. Among several quantities we calculate, we pay special attention to the pair-distribution function g(r), r being the interatomic distance, the bond orientational parameter W_6, and the frequency spectrum F(ω),ω being the vibrational frequency. The behavior of g(r) confirms the absence of the LRO. On the other hand, the behaviors of W6 for the nearest-neighbor atoms show the existence of the SRO in the form that the nearest-neighbor configurations are icosahedral as expected for these glasses. Interesting results are found in F(ω) in the sense that, in some glasses, the peaks appear in F(ω) at almost the same ω at the peak position in the case of an fcc crystal. From the analyses of W6 for atoms in the second-neighbor shell of each central atom, we find that the origin of the peaks in F(ω) comes from the cubic-like configurations of the atoms in the second-neighbor shell. We discuss this problem in detail and propose that F(ω), which is a macroscopically-observable quantity, is used as a measure to detect the degree of the IRO.

(Received July 4, 2005; accepted July 21, 2005)

Keywords: Glass, Simulation, Interatomic potential

1. Introduction

The absence of long-range order (LRO) and the existence of short-range order (SRO) are characteristic features common to all glasses and amorphous solids. Here, the term LRO is used to indicate that the atomic configurations are specified by the periodicity as found in crystals, while the term SRO is used to denote that the positions of nearest-neighbor atoms around a given atom in a disorderd system are almost identical to those in a corresponding crystal. Therefore the intermediate-range order (IRO) is expected to be a deciding factor in distinguishing one disordered system from another. Here, we use the term IRO as reprensenting the order in the atomic distributions beyond the nearest neighbors.

The purpose of the present paper is to propose a way detecting the IRO by studying the local symmetry of atomic configurations beyond the first-nearest neighbor. For this porpose we carry out rapid quench simulations to construct glassy structures by means of molecular dynamics method. The subjects we pay attention to include (1) the glass structure of the Lennard-Jones (LJ) system and

* Corresponding author: ysano@rk.phys.keio.ac.jp

of the Stillinger-Weber (SW) system, (2) quench rate dependences of the structures both from the point of view of macroscopic properties and microscopic strucrues through the glass transition. The reason why we study the SW system in addition to the LJ system, is to find if there is any common features in glasses of di_erent nature such as those with potentials leading to close-packed structures and those with potentials causing relatively open structures. We calculate several physical properties; the pair distribution function g(r) as structural properties, the frequency spectrum F(ω) for studying vibrational properties, the bond orientational parameter W6 to investigate local symmetries of atomic configurations in the first and second shell around a given atom.

In section 2 we describe our model and method, while the results are presented in section 3. Finally summary is given in section 4.

2. Model and method

We use the constant-pressure MD simulation method by Andersen [1] to study two model systems composed of 864 spherical particles; in one system, atoms interact with one another via 12-6 Lennard-Jones pair potential and in another system, atoms interact via Stillinger-Weber pair potential modified by Nos´e and Yonezawa [2]. Note that an LJ system leads to a closest-packed crystalline structure such as an fcc lattice at low enough temperatures, while an SW system leads to a relatively open crystalline structure such as a bcc lattice. For our SW system, we use the following pair potential which has been modified from the original three-body SW potential [3,4] so as to realize a bcc structure in the crystalline phase. In our simulations, the atoms are placed in a simulation cell with periodic boundary conditions. The calculations are conveniently performed in dimensionless variables by scaling the energy in ε, length in σ mass in M, temperature in ε/k_B, pressure in ε/σ^3, and time in $(M\sigma^2/\varepsilon)^{1/2}$, where ε and σ are the potential parameters of the Lennard-Jones potential, M is the atomic mass, and k_B is the Boltzman constant. The magnitudes of the units relevant to the argon are taken from the paper of Dangaard Kristensen [5] ε/k_B = 118K, σ = 3.84Å atomic mass $M_0 = 0.66\times10^{-22}$g, t_0 = 2.44ps, a time step for integration is taken to be Δt* = 0.0023 in reduced unit which corresponds to 0.5×10^{-14}s for argon. We choose the pressure P* = 1. In order to construct different initial conditions, we heat an fcc crystal from T* = 0.1 to T* = 4.0, and then anneal the system at T* = 4.0 for the time duration of various timesteps. For two different potentials we cool the initial systems down to T* = 0.2 with three quench rates; $Q_A = 4.2 \times 10^{10}$K/s, $Q_B = 4.2 \times 10^{11}$K/s and $Q_C = 4.2 \times 10^{12}$K/s.

$$\phi(r^*) = \begin{cases} 8.56438\left(\frac{1}{r^*}-\frac{1}{r^*}\right)\exp\left(\frac{1}{r^*-1.8}\right) & [r^*<1.8] \\ 0 & [r^*>1.8] \end{cases} \quad (1)$$

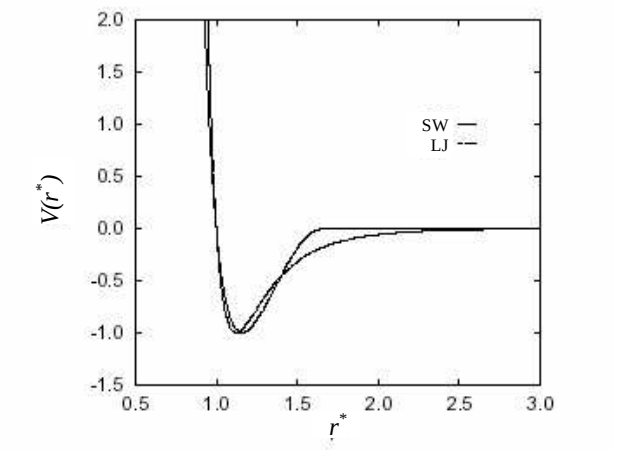

Fig. 1. The Lennard-Jones potential is presented by dotted curve, while the Stillinger-Weber potential defined by Eq. (1) is shown by solid curve, where r* = r/σ.

3. Results

3.1 Macroscopically observable properties

In this subsection, we study some of macroscopically observable properties such as volume V* and pair distribution function g(r*). The left side of Fig. 2 shows the V * -T* relation in the LJ system, where V * is the volume per atom. For the Q_A, a discontinuous decrease of volume is observed between T* = 0.3 and T* = 0.2, indicationg crystallization through the first-order transition. For higher quench rates Q_B and Q_C, on the other hand, the volume decreases continuously all the way in the process down to T* = 0.2, which shows freezing without forming crystal, suggesting the formation of glasses. In the case of an SW system, the relation is shown in the right side of Fig. 2. With all quench rates Q_A, Q_B and Q_C, the volume decrease continuously down to T* = 0.2, suggesting that the systems become glassy state.

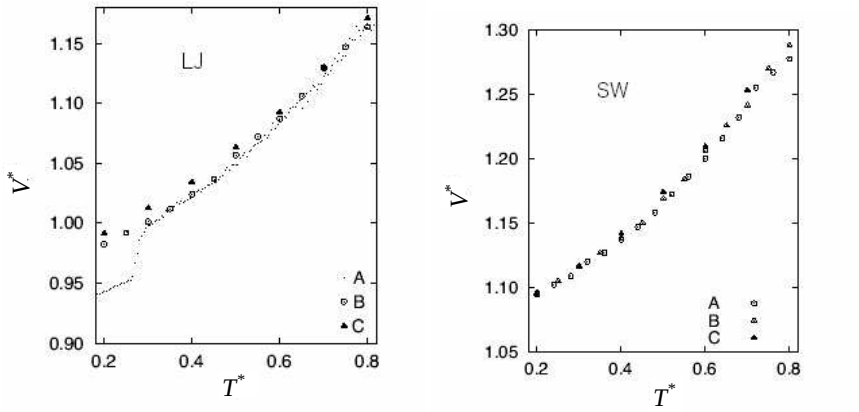

Fig. 2. The right figure shows volume versus temperature in the LJ system on quenching with quench rate Q_A, Q_B and Q_C by the dots, the open circles and the solid triangles respectively. The left figure shows the result in the SW system, in which the volume decrease continuously for all quench rates.

Fig. 3 (a) and (b) show the pair distribution function g(r*) for the quench rates Q_A and Q_B respectively in the LJ system. The peaks at the low temperature (T* = 0.2) in Fig. 2 (a) appear in the positions of the characteristic peaks of an fcc crystal, thus confirming the occurrence of crystallization in addtion to the result of the V * -T* relation. Fig.3 (b) for the quench rate Q_B in the LJ system presents that the atomic configurations are disordered all the temperatures. There appear in particular at low temperatures the splitting of the second peak, which is a characterictic feature of g(r*) for glasses. For the quench rate QC as well as for Q_A, Q_B and Q_C in the SW system, g(r*) behave the same manner as Fig.3 (b), which confirms the formation of glasses.

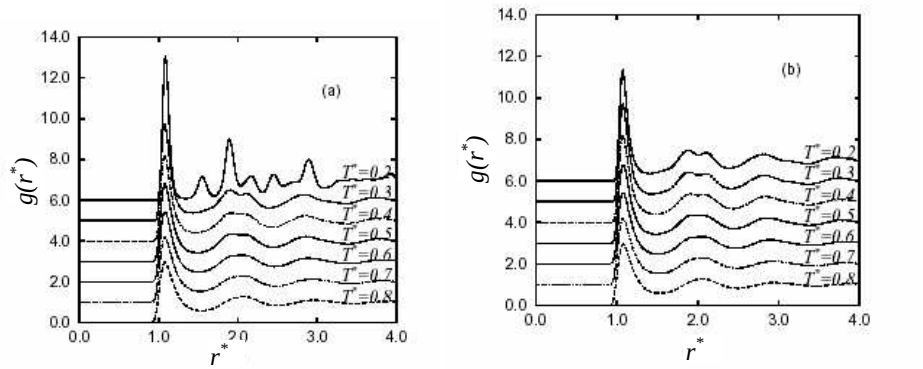

Fig. 3. The pair distribution function g(r*) between temperature T* = 0.8 and 0.2. (a) g(r*) with quehch rate Q_A, for which there appear peaks characteristic of the crystallization at T* = 0.2. (b) g(r*) with QB, a glass-forming quench rate.

3.2 Frequency spectrum of vibrational modes

In order to investigate the vibrational motions of atoms in the glassy states, we calculate the velocity autocorrelation function (VAF) υ(t), defined by

$$\upsilon(t) = \frac{\left\langle (1/N)\sum_i v_i(t_0+t)\cdot v_i(t_0)\right\rangle t_0}{\left\langle |v(t_0)|^2\right\rangle t_0} \tag{2}$$

and the frequency spectrum F(ω) which is the Fourier transformation of the VAF given as follows;

$$F(\omega) = \frac{6}{\pi}\int_0^\infty \upsilon(t)\cos(\omega t)dt, \tag{3}$$

where v_i is the velocity vector of the ith atom at t, and the brackets h··i denote the average over initial conditions $\{t_0\}$.

Fig. 4 shows the F(ω*) of each quench rate in the LJ system. The left side of Fig. 4 presents the results with quench rate QA at T* = 0.3 and T* = 0.2. Note that according to the results of V * - T* relation and g(r*), the first-order transition takes place at temperature slightly lower than T* = 0.3. Though there is no peak at T* = 0.3, there appears at T* = 0.2 a wide peak around frequency ω* = 13 which corresponds to the distinct peak in F(ω*), as shown by a broken curve, of an fcc crystal under P* = 1.0 and T* = 0.2.

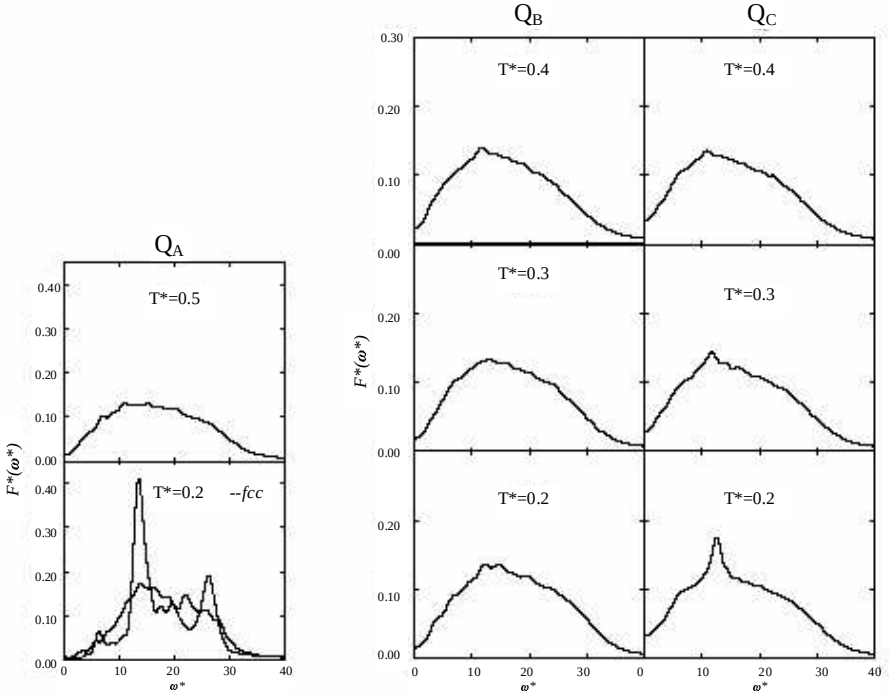

Fig. 4. Figures on the left show frequency spectra F(ω*) versus ω* for Q_A at T* = 0.3 and T* = 0.2, between which the occurrence of the first-order transition is indicated. The broken curve corresponds to an fcc crystal at T* = 0.2 with the same volume as for the Q_A. The three figure in the center show the F(ω*) for the Q_B and on the right the results of Q_C. The glass transition occurs at about T* = 0.4.

The right side of Fig. 4 shows the results with quench rate Q_B and quench rate Q_C, both of which are glass-forming quench rates and the glass transition occurs at about T* = 0.4. There is no peak in the F(ω*)at T* = 0.4 similar to F(ω*) of liquid state. As the temperature decreases, with both

quench rates, the peak appears gradually at ω* ~ 13 which corresponds to the peak position of fcc crystal. It shows that the higher the quench rate, the higher the peaks grow up. As for the SW system, the calculated results of F(ω*) are presented in Fig. 5, which show the behaviors similar to F(ω*) for Q_B and Q_C in the LJ system. In the SW system, the peaks appear at ω* ~ 9, which corresponds to the peak position of a bcc crystal as illustrated by a broken curve in the right-bottom figure. These results of F(ω*) are very interesting in following respects; In spite of the fact that, from g(r*), the atomic configurations are shown to be disordered, there appears a peak at the same frequency as the peak position of bcc crystal. The appearance of this peak suggests that there exist some aspects of cubic symmetry, which is contradictory to the concluions drawn from g(r*). We try to pin down the origin of the peak in F(ω*) by investigating the local symmetry in a succeeding section.

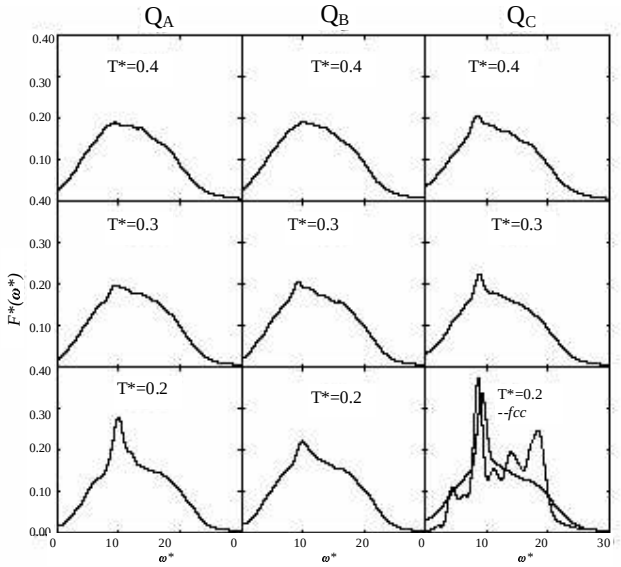

Fig. 5. From left to right, the results of Q_A, Q_B and Q_C in the SW system are presented. The broken curve in the bottom right shows F(ω*) of a bcc crystal under P* = 1 and T* = 0.2.

3.3. Local symmetry of atoms

We use the bond orientatilnal parameter W_6 as a quantity to calculate the local symmetry of atoms. This parameter is suitable for distinguishing the local icosahedral symmetry from the local cubic symmetry, which was introduced by Steinhardt et al [6], and modified by Yonezawa et al [7] to study the symmetry formed by a given group of atoms such as atoms in the first and second shell. Since the local idosahedral configuration is expected in disordered sysmtens such as liquid and glasses composed of isotropic atoms, this parameter is useful to examine the local symmetry. In the present paper, we calculate not only W6 parameters for atoms in the nearest-neighbor shell but also W6 parameters for atoms in the second-neighbor shell in order to investigate the symmetries of local atomic configurations beyond the nearest neighbor.

Symmetry of the first shell

In the nearest-neighbor shell of a given atom, the value of W6 is -0.169 for a perfect icosahedron, while the value of $|W_6|$ is about 0.013 for a cluster with crystalline symmetry, such as a simple cubic cluster, an fcc cluster and a bcc cluster. In order to investigate the local symmetry of atoms, we classify the atoms into three categories [7];

(1) atoms with icosahedral symmetry, where an atom is regarded as having icosahedral symmetry when $0.05 < W_6 < 0.17$;
(2) atoms with cubic symmetry, where an atom is regarded as having cubic symmetry when $0.005 < |W_6| < 0.02$;
(3) the other atoms.

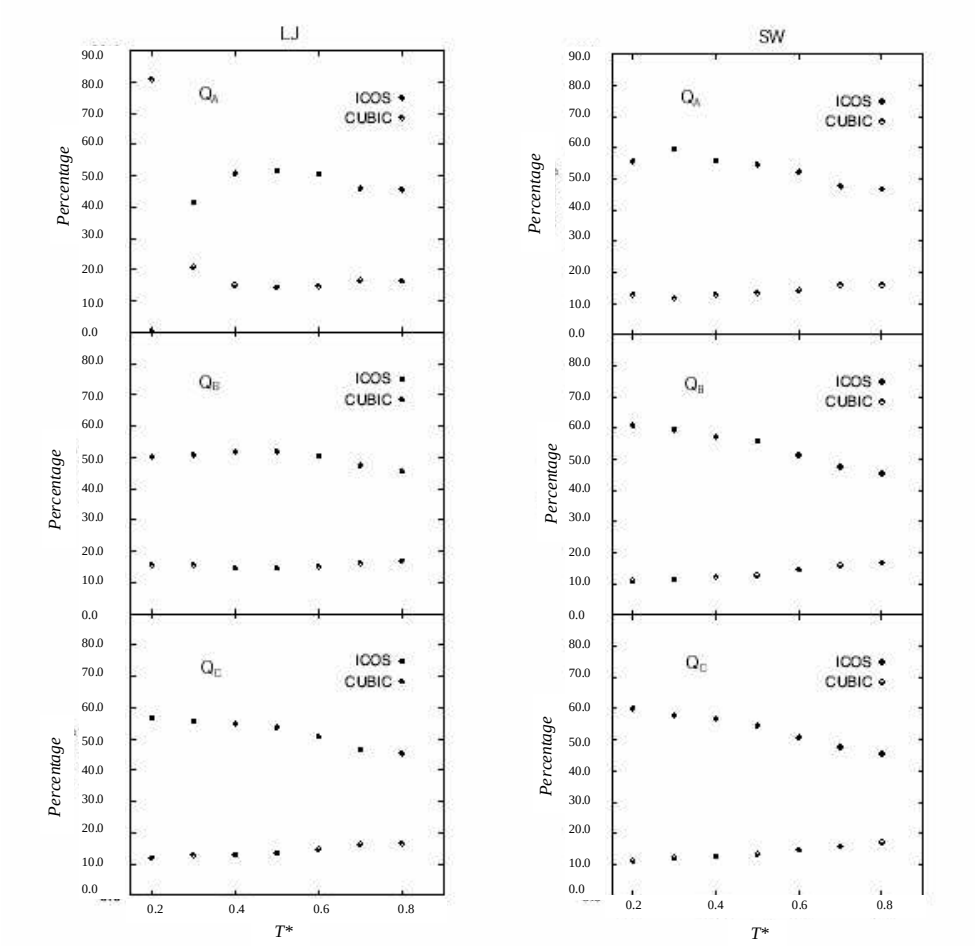

Fig. 6. The proportions of atoms with the icosahedral (the solid circles) and cubic symmetry (the open diamonds) in the first shell on the temperature reduction estimated from the bond orientational parameters W_6. The left side shows the results in LJ system, while the left side shows that in SW systems; from top to bottom, the processes of Q_A, Q_B and Q_C are shown respectively.

Figs. 6 show the proportion of atoms with icosahedral and cubic symmetries as far as the nearest-neighbor shell is concerned. In Figs. 6, the results of the LJ and SW are respectively demonstrated on the left and right. For each case, the process of quench rate Q_A, Q_B and Q_C are illustrated from top to bottom. Let us first look at the top-left figure for Q_A in the LJ system. The number of atoms with local icosahedral symmetry decreases suddenly between T* = 0.3 and T* = 0.2, while the number of atom with local cubic symmetry increases drastically, which reflects the occurence of crystallization around this temperature. On the other hand, we can observe in all the other five figures that the local icosahedral symmetry remains intact all the way down to T* = 0.2. This behavior is consistent with the conclusion drawn from the V* - T* relation and g(r*) that a glass is formed in each of these five cases. This persistence of local icosahedral symmetry in these glasses, however, contradicts with the appearance of a peak in F(ω*). In order to solve this problem, we study the symmetries with respect to the atomic configurations in the second shell of each atom.

Symmetry of the second shell

We use the modified W_6 to calculate symmetry formed by atoms in the second shell. The value of the W_6 is -0.169 for the second shell in a perfect icosahedral structure, while that of the $|W_6|$ in a perfect cubic structure is 0.013, this parameter is useful to distinquish the icosahedral and cubic symmetries concerning the atoms in the second shell as well. Fig. 7 show the distributions of W_6 at

T* = 0.8, T* = 0.4 and T* = 0.2 in the second shell where the distribution is taken only over those atoms whose nearest-neighbor atoms form local icosahedral symmetry. Here, T* = 0.8, T* = 0.4 and T* = 0.2 respectively correspond to a liquid state, a temperature near the glass-transition temperature, and a glassy state. The left side in the Fig. 7 represents the results with quench rates Q_B and Q_C in the LJ system, while the right side shows the results with Q_A, Q_B and Q_C in the SW system. All the shape of the distribution have the peak at $W_6 \sim +0.01$ which corresponds to cubic symmetry in the second-neighbor shell. We can see that there are no temperature dependence in both cases.

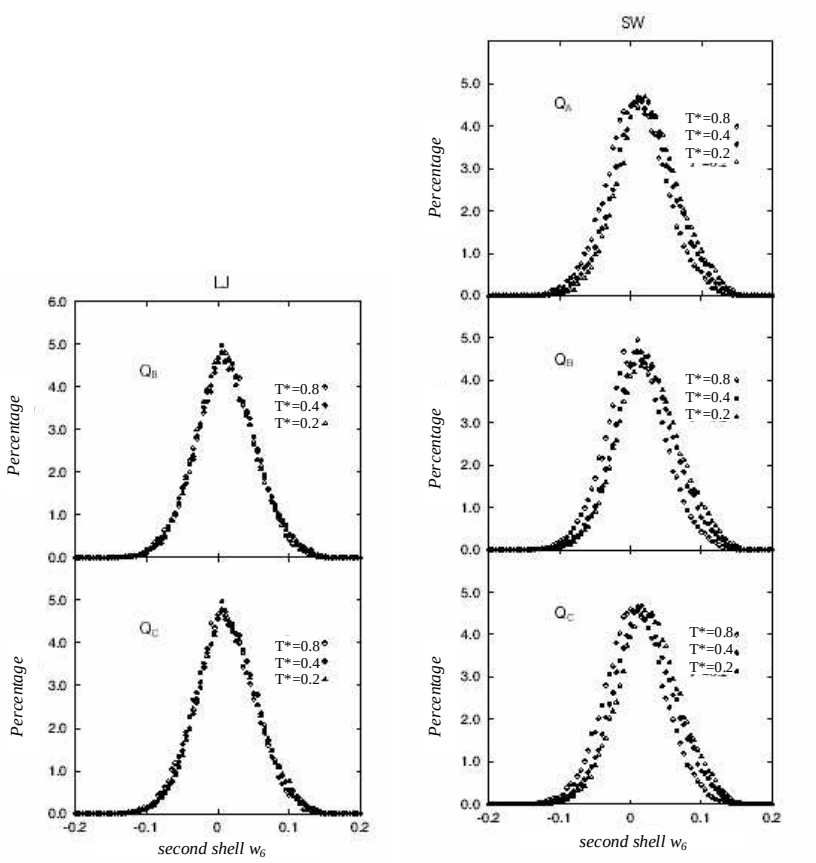

Fig. 7. The distribution of W_6 for the second shell at T* = 0.8, 0.4 and 0.2, for which the atoms have the local icosahedral symmetry in the first shell. The left side presents Q_B and Q_C in the LJ system, while the right side presents Q_A, Q_B and Q_C in the SW system.

As for the quench-rate dependence, the results show no dependence in the LJ case while a slight dependence is descernible in the SW case. It has been argued in our previous study [8]~[12] that, when the quench rate is very high, the atoms do not have enough time to search for low-energy configuration over a wide space, but instead they are solidified by minimizing energy in the immediate vicinity of each atom, thus yielding the icosahedral configuration around each atom. This is the reason why we have the larger number of atoms with the icosahedral symmetry in the first shell when the quench rate is the higher. This tendency can be seen more clearly in Fig.8 where the number of atoms with icosahedral symmetry in the first shell is presented versus quench rate both for the LJ and SW system.

These results however seem to be totally contradictory to the fact that the peak appears in $F(\omega^*)$ of glasses at the same frequency as the typical peak position in $F(\omega^*)$ of an fcc crystal. Another problem about the local icosahedral configuration is that it cannot be packed in a consistent manner over the whole space. These problem are all resolved by our results as shown in Fig. 7,

which illustrates that, even when the local symmetry of atoms in the first shell is icosahedral, the atomic configurations of atoms in the second shell have cubic symmetry. In other words, each cluster including atoms up to the second shell has a shape with cubic symmetry, and accordingly the close packing over a wide space is possible and the peak in F(ω*) showing a vestige of cubic crystals is accounted for.

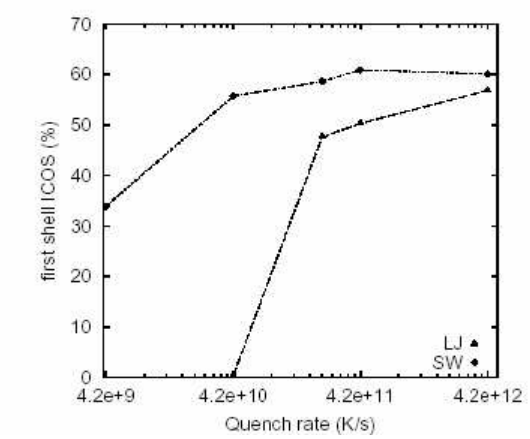

Fig. 8. The relations between the quench rate and the proprtion of the icosahedral atoms in the nearest-neighbor shell at the temperature T* = 0.2. Open triangles show the results in the LJ system while open circles show the SW system.

4. Summary

By using constant-pressure molecular dynamic simulations, we have prepared glasses by quenching liquids. We adopted model systems composed of 864 spherical particles with the Lennard-Jones potential as well as the Stillinger-Weber potential. We have analyzed the structures of the glasses both from the view point of macroscopic and microscopic properties in detail; we have discussed the SRO and LRO by calculating the bond orientational parameter W_6 and the pair distribution function g(r*). In particular, interesting results have been found in frequency spectrum F(ω*). In spite of the fact that the system is glassy, the peak appears in F(ω*) at almost the same frequency ω* as the peak position in the case of a cubic crystal both in the LJ system and in the SW system. By calculating W6 for atoms in the second-neighbor shell of each atom, we have found that the peak in F(ω*) arises from the cubic-like configurations of the atoms in the second-neighbor shell.

By taking the above-described results into account, we propose that the frequency spectra F(ω*) of vibrational modes can be used as a measure for the order in the atomic configurations beyond the nearet-neighbor shell of each atom.

References

[1] H. C. Andersen, J. Chem. Phys. **72**(4), 2384 (1980).
[2] S. Nos´e, S. Sakamoto, F. Yonezawa Zeitschrift fur Physikalische Chemie Nemie Folge, Bd. **156**, S.91 (1988).
[3] F. H. Stillinger, T. A. Weber J. Chem. Phys **70**(11), 4879 (1979).
[4] F. H. Stillinger, T. A. Weber J. Chem. Phys **68**, 3837 (1978).
[5] W. Damgaard Kristensen, J. Non-Cryst. Solids **21**, 303 (1976).
[6] P. Steinhardt, D. R. Nelson, M. Ronchetti Physical Review B **28**, (1983)
[7] Fumiko Yonezawa Solid State Physics. **45**, (1991).
[8] M. Kimura, F. Yonezawa, in "Topological Disorder in Condensed Matter"(F.Yonezawa and T. Ninomiya, eds.). Springer, Computer Glass Transition, 1983.
[9] S. Nos´e, F.Yonezawa, Solid State Commun. **56**, 1005 (1985).
[10] F. Yonezawa, S. Nos´e, S. Sakamoto, J. Non-Cryst. Solids **95**(96), 83 (1987).
[11] F. Yonezawa, S. Nos´e, S. Sakamoto, J. Non-Cryst. Solids **95**(96), 373, (1987).
[12] F. Yonezawa, S. Nos´e, S. Sakamoto, Neue Folge **156**, 77 (1988).